Switching characteristics of tunneling injection and diffusion injection single quantum-well semiconductor optical amplifiers

Cristiano M. Gallep and Evandro Conforti.

Departamento de Microonda e Óptica
Faculdade de Engenharia Elétrica e de Computacão – Unicamp

ABSTRACT

A simple model for quantum well semiconductor optical amplifier simulation is presented. Carrier population transients in the separate confinement heterostructure and in the unconfined (above) and confined (inside) states of the quantum well are considered. Simulations results for pure tunneling and pure diffusion cases of the injected current in the switching action are presented. Switching times under 50ps are obtained for high input optical power (100μW) and a 0.3-1mA current step.

1 - INTRODUCTION

The semiconductor optical amplifier (SOA) is a promising device for add-and-drop links and wavelength routing. In addition, the SOA can be employed as an optical switch due to its small size, wide bandwidth and the potential to be integrated with other electronic and optical devices [1]. Present day limitations of a SOA switch are the high price and limited isolation between WDM (wavelength division multiplex) channels [2]. However, angle-facet S-bend SOA switches can overcome the last limitation, providing a large optical extinction ratio (optical *off-on* ratio) of 70 dB with a fiber to fiber gain of 20 dB [3]. Modern SOA with active cavity based on quantum well structures can provide wide gain band, high saturation power, good small signal gain and fast gain recovery, factors that make this devices a promising tool for the accomplishment of totally optical processing sub-systems

Computer simulation of numerical models for such devices is an important tool to the design of more complex systems and prediction of high speed optical data links performance. In this work, a simple and efficient model for quantum-well semiconductor optical amplifier (QW-SOA) is presented with some simulations results. The rate equations account to the carrier populations in the SCH region and in the states above (unconfined) and inside (confined in) the well. Also, a photon population equation is considered.

2 - QW-SOA CHARACTERISTICS

The high-speed semiconductor lasers dynamics have been conventionally modeled using a pair of coupled first-order linear differential equations, usually called *rate equations*. In that approach, one equation governs the electronic carrier density and other one governs the photon density inside the cavity. The non-linear dependence of the optical gain with the photon density is generally introduced by a gain compression factor. In practice, the dynamic response of bulk-type active cavity devices are limited by RC parasites, heating, carriers relaxation times and maximum power supported by the structure. In the peculiar case of QW structures, the carrier transport mechanisms are very important to the dynamic performance. In that way, the QW structural optimization should also be done considering the relationship of the well's width and number; the barrier's height and width; the composition types of SCH (separate confinement heterostructure); the amount of bi-axial forces in the crystalline media and the type and amount of doping in the active layers.

The quantum-well structure provides a significant reduction of the valence band carrier's effective mass [4], allowing operation with lower threshold current, reduced Auger recombination, increased differential gain and modulation band. The largest attractiveness of those devices are its potentialities of high dynamic response operation, due to the barrier's carrier reservoirs and carrier tunneling. Using an optimum design, gain recovery time less than 10 ps was obtained in MQW optical amplifiers [5]. In an QW structure, the optical field confinement in the active area is very small, due to its small dimensions (relatively to the light wavelength). In those case a high insertion loss (~95%) is expected. Even so, the material gain is 50% larger in relation to common devices, when the wells are under presence of bi-axial forces [6]. Due to the quantum process involved in the electronic carriers transport, gain restoring times of pico-seconds can be obtained.

The Auger-type is one of the predominant processes of non-radioactive recombination in optical fiber communications lasers, affecting its gain linearity and modulation response. This process involves four states of particles (three elétrons (*e*) and a hole (*h*), two *e* and and two *h*, etc.). The resultant *e-h* recombination energy is transferred to another carrier (an electron or hole), that becomes excited, achieving a higher energy state in the corresponding band [7]. This *hot-carrier* then relaxes again to the ground state, losing energy through vibrations in the crystalline structure (phonon). The Auger recombination can be reduced 10 times in QW structures, in relation to the conventional ones. Such a fact could be explained by the reduction, in comparison to structures of matched crystalline layer, of the carrier effective mass [8]. Even so, the Auger recombination is still one of the most serious problems in SQW-lasers (single-quantum well) with InGaAsP-InP structure, in spite of been its coefficient ($C = 8.10^{-31} cm^6/s$) three orders of magnitude smaller than of conventional structure devices ($10^{-27} cm^6/s$). In MQW structures with injection of carriers by tunneling, the Auger recombination is still smaller, due to the reduction of the *hot carriers* effects.

In resume, we can relate that the main processes influencing the modulation answer in QW-lasers are [9]: photon lifetime, spectral hole burning, carrier heating and transport of carriers. The main mechanisms of carrier transport are the transport through the SCH, the carrier capture by the quantum well, the carrier escape (or termionic emission) from the well, and carrier tunneling. It can be assumed that all holes are captured by the first well, due to its small time of capture, and later transported through the QW structure by termionic emission, diffusion over the barrier and capture for the following well or by direct tunneling through the barrier. For an optimized barrier, the barrier diffusion times and the capture by the next well are worthless in relation to the term-ionic emission time.

The carrier escape process from the quantum well depends on the confined carrier's energy distribution. Comparative results between simulation and modulation response for M(multi)QW-lasers show a fast electron heating in the electronic injection case. That heating accompanies the carriers density modulation and acts against its effect in the optical gain, taking to a dynamic answer degradation [10]. The cooling of the *e-h* pairs created during the absorption is dominated by the phonon interaction scattering. Times of few pico-seconds were observed for that phenomenon [11]. Using the fast replacement of carriers, QW-SOA can be implemented for high power operation and with lower pattern dependence [12].

The carrier tunneling mechanism (in major part electrons) through the barriers in QW structures can be used to (besides decreasing transport times) decrease the hot-carrier effects in the optical-active well. For that, the electron is injected in the well with an energy close to the photon energy, in those called TI-lasers (*Tunneling Injection*). The injection is made in a superior rate to that of the stimulated emission, maintaining the electronic distribution in the quasi-Fermi level, even for high bias currents [9].

3 - QW-SOA MODEL

To implement a simple QW-SOA model, a four rate equations approach is used in order to account to the carrier population in the SCH, N_{SCH}; in the unconfined state above the well, N_{ab}; in the confined state inside the well, N_{in}; and for the photon density S. It is presented in (1) to the single-well case, where:

- N_{SCH} receives carriers from the injected current and loses them by tunneling directly to N_{in} or by diffusion to N_{ab}. Here, carrier recombination are neglected.
- N_{ab} receives carriers from that diffusion current of N_{SCH} and from carrier escape of N_{in}, and loses them by carrier capture to N_{in} and spontaneous emission.
- N_{in} receives carriers from that tunneling current of N_{SCH} and from carrier capture of N_{ab}, and loses them by carrier emission to N_{ab} and by spontaneous and stimulated emission.
- S is amplified or absorbed, depending on the N_{in} conditions.

$$\begin{aligned}
\frac{\partial}{\partial t}N_{SCH} &= \frac{J}{q\cdot L_{SCH}} - N_{SCH}\left(\frac{f}{\tau_t}+\frac{1-f}{\tau_d}\right)\\
\frac{\partial}{\partial t}N_{ab} &= N_{SCH}\frac{1-f}{\tau_d}\frac{L_{SCH}}{L_W}+\frac{N_{in}}{\tau_e}-N_{ab}\left(\frac{1}{\tau_c}+\frac{1}{\tau_{n_{ab}}}\right)\\
\frac{\partial}{\partial t}N_{in} &= N_{in}\frac{f}{\tau_t}\frac{L_{SCH}}{L_W}+\frac{N_{ab}}{\tau_c}-N_{in}\left(\frac{1}{\tau_e}+\frac{1}{\tau_{n_{in}}}\right)-\Delta S\cdot\frac{A_g}{V_W}\\
\frac{\partial}{\partial t}S &= S\cdot\Gamma_W\exp(g\cdot L_z)
\end{aligned} \qquad (1)$$

where f is the factor for injection division between pure tunneling (f=1) and pure diffusion (f=0), V_w is the well volume, A_g the optical guide area and τ_n is the carrier lifetime, defined as:

$$\tau_{n_i}(N_i) = \frac{1}{A+BN_i+CN_i^2} \qquad (2)$$

where A, B and C are the recombination factors representing, respectively, defects and traps, spontaneous emission and Auger recombination; i can be *ab* or *in* (referent to N_{ab} or N_{in}) and g is the net gain obtained by [13]:

$$g(N_{in}) = \begin{cases} G_0 \ln\left(\dfrac{AN_{in}+BN_{in}^2+CN_{in}^3}{AN_{th}+BN_{th}^2+CN_{th}^3}\right), & \text{for } N_{in} \geq N_{th} \\ -\alpha, & \text{for } N_{in} < N_{th} \end{cases} \qquad (3)$$

The other parameters and its values are listed in the Table I.

TABLE I: SIMULATION PARAMETERS

Parameter	definition	value
L_{sch}	SCH height	0.1 μm
L_w	well height	5 nm
L_z	cavity length	100 μm
w	cavity width	3 μm
N_{th}	threshold carrier dens.	9.10^{23} cm^{-3}
τ_t	tunneling time	1 ps
τ_d	diffusion time	1 ps
τ_e	escape time	1 ns
τ_c	capture time	10 ps
G_0	linear gain	380000/m
α	attenuation	100000/m

4 - SIMULATION RESULTS

To solve the rate equations in (1), the usual fourth-order Runge-Kutta method is applied. The presented results are for the single-well case, where is assumed an non-z discretization. Such a way, the cavity length (100μm) limits the time steps, in order to respect the wave travelling time inside the crystal. Therefore the events with less duration than that (~1ps) will be neglected.

For the pure diffusion injection case (f= 0), the CW values for carrier concentrations in the confined and unconfined states, for three values of optical input power (1, 10 and 100μW), in relation to the bias current, are shown in Fig.1. The same results are shown in the Fig.2 for f = 1 (pure tunneling injection case). In these two figures it is visible that the final carrier concentration inside the well, N_{in}, are stable for high values of the injected current. For high input optical power (100μW), N_{in} is higher, comparatively to low input powers, in case of sub-threshold bias current. Above threshold (see Table I), all N_{in} values tends to an equilibrium (~10^{24}/cm^3) to all f-cases, but with low values to the high optical input power case, showing the gain saturation aspect of light amplification. This fact, gain saturation, could also be analyzed looking at the net gain in Fig.3: very high gain (18.2dB) to low input optical power (P_{in}= 1μW), moderate gain (8.6dB) to moderate input optical power (P_{in}= 10μW) and a net attenuation (-0.5dB) to high input optical power (P_{in}= 100μW). For the population above the well, N_{ab}, those observations about saturation level are also valid. But these levels are not the same all the f-cases. For f = 0 (Fig.1), a higher population is observed for a high input optical power, a tendency to rise up with bias current. This behavior could be explained by the fact that in this case, all carriers pass into the unconfined state before be captured by the well. As many carriers are been consumed in the confined state for high input power, a higher density in the unconfined state is necessary to feed the confined state conveniently.

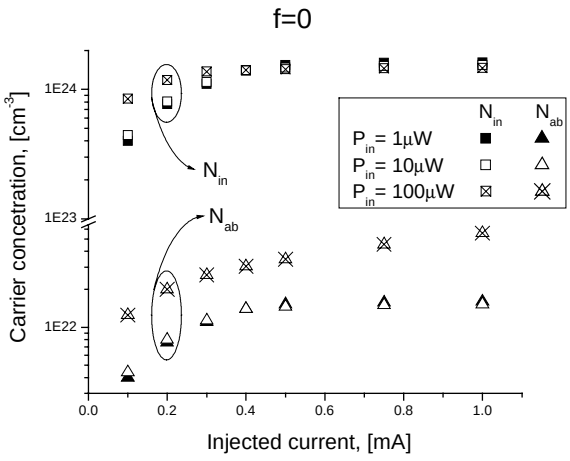

Figure 1. Final carrier concentration for f = 0 (pure diffusion injection).

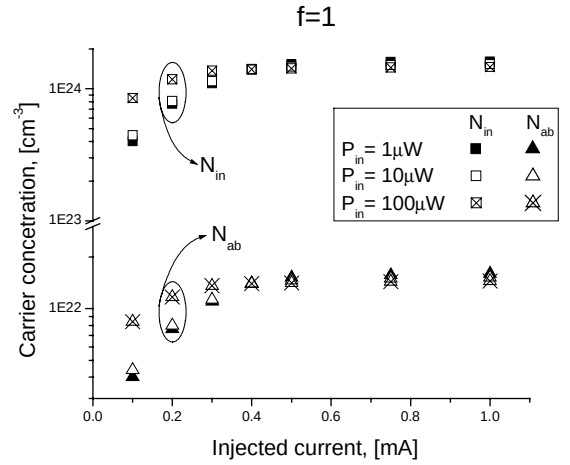

Figure 2. Final carrier concentration for f=1 (pure tunneling injection).

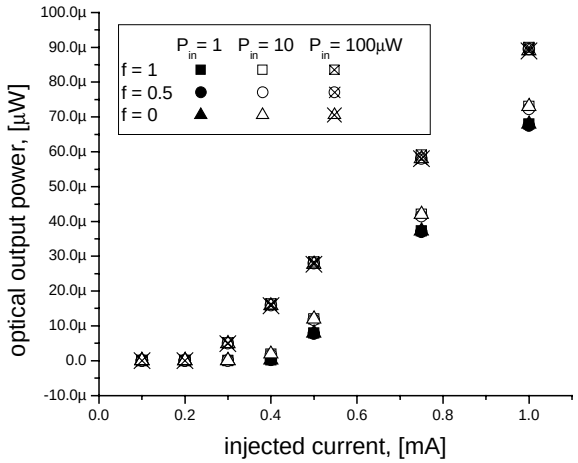

Figure.3. Optical output power for three injection cases versus current injection.

As the f factor rises up to 0.5 (graphic not shown here), the N_{ab} population tends to a common value for all saturation conditions, even more in above threshold conditions. Below threshold, high input powers causes high population densities, since half of the carrier replenishment for N_{in} is made by carrier capture from N_{ab}. For f = 1 (Fig.2) the N_{ab} level decrease, since only carrier tunneling feeds directly N_{in}, and N_{ab} receives carriers only by carrier escape from the state inside the well. Besides not been optical active for the interest spectrum, the N_{ab} population is important due its function as a carrier reservoir for very fast carrier replenishment, enabling operation without the pattern-dependence problem. This characteristic can be used in all-optical processing, since an auxiliary optical channel can control N_{ab} population, adding/consuming electronic carriers by optical absorption/amplification.

In Fig.4, the transient responses of the output optical power and carrier concentration inside and above the well are shown for a instantaneous (<1ps) current step (0.3-0.6-0.3 mA), for an example with an optical input power of 1μA (unsaturated amplification) and pure tunneling injection (f = 1). The carrier concentrations are out of scale, just for qualitative analysis. As shown in this figure, the N_{in} population rises up after the current step-up due carrier tunneling to the quantum well. As soon as N_{in} is up to the threshold value, the optical amplification occurs and the ON-state switch is achieved. With the N_{in} growth, the carrier escape mechanism acts in order to feed the N_{ab} population, which rises up until a stable value. At these CW state, permanent spontaneous emission occurs as a population limitation action. When the current falls down, N_{in} and N_{ab} are consumed by carrier spontaneous emission and N_{in} is feed by carriers stocked in N_{ab}. To the pure diffusion case (f=0), significant modifications on the populations transitories occur, since the injection is made only by diffusion.

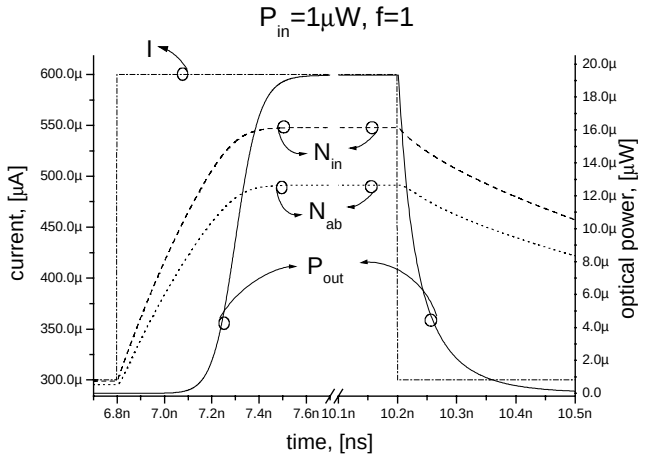

Figure 4. Switching characteristics for f=1 (pure tunneling injection) and P_{in}=1μW (unsaturated operation)

In Fig.5, the transient responses are shown, as in Fig.4, but now for the pure diffusion injection case (f = 0). After the injected current step, the carrier concentration in the unconfined states above the well (N_{ab}) rapidly rises up and starts to feed the confined state inside the well (N_{in}) by carrier capture. As N_{in} supplants the threshold condition, the optical signal is amplified by stimulated emissions with an optical gain proportional to a logarithmic relation between N_{in} and the threshold condition (3). The carrier concentrations N_{ab} and N_{in}, in Fig.4 and 5 assume numbers around, respectively, 10^{22}cm^{-3} and 10^{24}cm^{-3}. The total carrier concentration

(inside plus above the well) consumed in spontaneous recombination, is around $10^{21}cm^{-3}$, and rises up with the total carrier population. As the injected current falls down, the N_{ab} quickly vanishes, but N_{in} takes longer to fall, since after been below threshold condition, this population is only consumed by carrier escape to the states above the well and spontaneous emission.

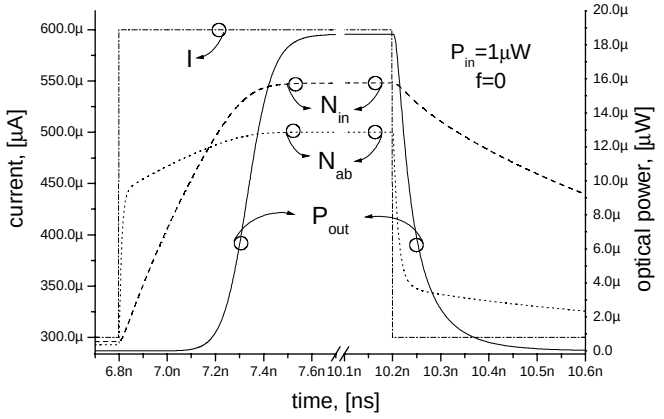

Figure 5. Switching characteristics for pure diffusion injection (f=0) and P_{in}=1μW (unsaturated operation)

The variation of the switching times and net optical gain at ON-state, with the injected current step (starting from 0.3mA) and for three injection schemes, pure tunneling (f=1), pure diffusion (f=0) and intermediate (f=0.5) injection conditions is shown, for P_{in}=1μW, in Fig.6. The intermediate injection configuration appears as the fastest on-switching for small (0.1mA) current steps. For higher steps, no significant differences are observed between the three different configurations, and the off-on time decreases from 2ns to less than 300ps. The net optical gain has a saturated profile for current steps higher than 0.3mA for all the three injection schemes, fact more evident for f = 0.5.

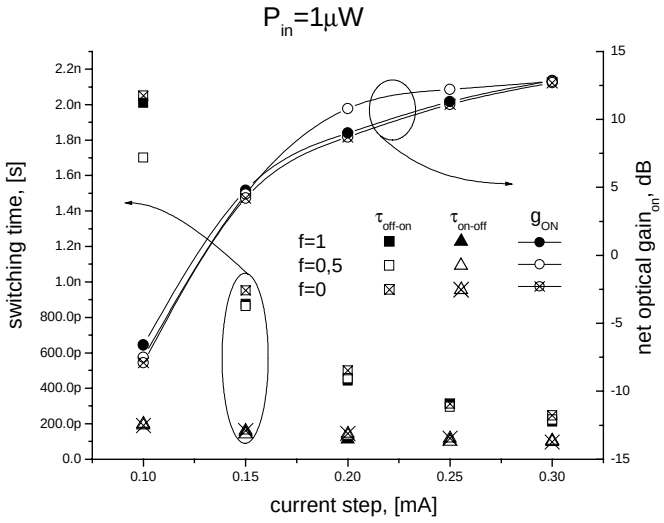

Figure 6. Switching times versus injected current step for P_{in}=1μW and three injection configurations: pure diffusion (f=0), intermediate (f=0.5) and pure tunneling (f=1).

Fig.7 and 8 show the current step response for two injection cases, as in Fig.4 and 5, but now for P_{in}=100μW (saturaded amplification). For this level of optical input power, higher switching velocities can be obtained, as shown in Fig.9. Fig.7 shows the pure tunneling injection case. In this case, after the current step-up the population inside the quantum well (N_{in}) increases by carrier tunneling through the confinement barrier. The population above the well (N_{ab}) increases by carrier escape from the well. As commented before, the amount of carriers consumed by spontaneous emission rises up with carrier concentration. With the current fall, N_{in} quickly drops down, been followed by N_{ab}, due spontaneous emission. For pure diffusion injection condition (Fig.8), the increase in the injected current causes an abrupt rise in N_{ab} by diffusion. Then, N_{ab} feeds N_{in} by carrier capture, and so this configuration should exhibit a slow switching operation. When the current drops down, N_{ab} is emptied since no more injection is done and the carrier population continues to be consumed by capture to the well and by spontaneous emission.

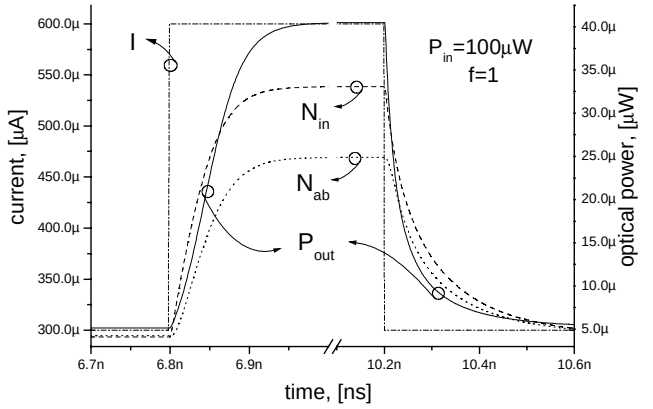

Figure 7. Switching characteristics for pure tunneling injection (f=1) and P_{in}=100μW (saturated operation)

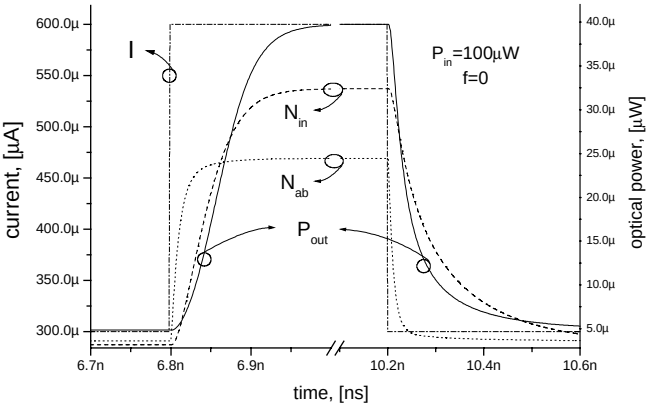

Figure 8. Switching characteristics for pure diffusion injection (f=0) and P_{in}=100μW.

In Fig.9, a resume of the switching operation characteristics with the injected current step (starting from 0.3mA) for P_{in}=100μW is shown. The ON-state net optical gain appears saturated by the high input optical power and tends to a upper-bound with the current step. No significant difference is found between the injection cases for the OFF-ON switching action, which has its time reduced from more than 170ps to less than 50ps with the current step increasing. A little difference (~10ps) appears in the ON-OFF beginning in 0.3 current step, due the carrier capture time. Its switching time achieves values under 80ps.

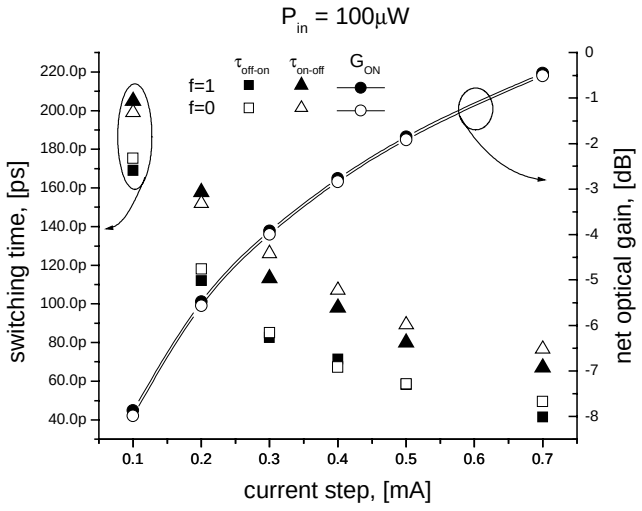

Figure 9. Switching times versus injected current step for P_{in}=100μW and two injection configurations: pure diffusion (*f*=0) and pure tunneling (*f*=1).

5 - CONCLUSIONS

A simple model for QW-SOA simulations has been presented. Preliminary results for the SQW case without space discretization were commented, with focus on the CW carrier population inside (confined) and above (unconfined) the well. Since the space discretization was not used, the population densities could be seen as an average inside the active cavity. Simulations results for the switching action were also presented. Switching times of less than 50ps were found for a saturated operation and significant step (0.3-1mA) of the injected current. Future works intend to implement such model using space discretization to allow the study of pulse amplification during its travel inside the cavity, considering also more than one optical channel, with propagation in inverse directions. Such approach could be very useful in the study and development of very fast optical switches. In order to simulate more than one single well, a pair of rate equations for N_{ab} and N_{in} in (1) must be used for each added quantum well. In this case, the terms that account to the SCH feeding appear in the equations for the first well carriers, linked to the other wells by tunneling and/or diffusion. All simulations results need an experimental validation. However, they are an useful tool in the investigation of the best device configurations before practical implementations.

This work is partially supported by FAPESP-CEPID, CAPES and MCT-Pronex. The initial part of this paper has been submitted to the 2001 International Microwave and Optics Conference.

6 - REFERENCES

[1] - Y. Shibata, Y. Yamada, K. Habara, and N. Yoshimoto, "Semiconductor laser diode optical amplifiers/gates in photonic packet switching", *J. Lightwave Technology*, Vol. 16, Nº 12, pag. 2228-2227, dec./1998.

[2] - N. A. Jackman *et. all*, "Optical cross connects for optical networking", *Bell Labs Technical Journal"*, pp. 262-281, Jan-March, 1999.

[3] - S. Kitamura *et. all*, "Angled-Facet S-bend semiconductor optical amplifiers for high-gain and large-extinction ratio", *IEEE Photonics Technology Letter*, Vol.11, N. 7, pp. 788-790, 1999.

[4] - J. P. Loehrb – "Physics of Strained Quantum Well Lasers" – Kluwer Academic Publishers, Massachusetts/EUA, 1998.

[5] - G. Eisenstein *et. all*, "Ultrafast gain dynamics in 1.5 μm multiple quantum well optical amplifiers", *Applied Physics Letters*, Vol. 58, Nº 2, jan./1991, pg. 158-161.

[6] - M. Asada *et. all* – "Gain and Intervalence Band Absortion in Quantum-Well Lasers" – *IEEE J. of Quant Electr*., Vol. QE-20, Nº 7, jul./1984, pg. 745-753.

[7] - G. P. Agrawal e N. K Dutta, *Semiconductor lasers*, 2ª ed., Van Nostrand Reinhold, 1993.

[8] - M. C. Wang *et. all*, "Measurements of nonradiative Auger and radiative recombination rates in strained-layer quantum-well systems", *Applied Physics Letters*, Vol. 62, Nº 2, jan./1993, pg. 166-168.

[9] - C. Tsai *et. all*, "A small-signal analysis of the modulation response of high-speed quantum well lasers: effects of spectral hole burning, carrier heating and carrier diffusion-capture-escape", *IEEE J. of. Quantum Electr*., Vol.33, Nº 11, nov./1997, pg. 2084-2096.

[10] - M. Grupen and K. Hess, "Severe gain suppression due to dynamic carrier heating in quantum well lasers", *Applied Physics Letters*, Vol.70, Nº 7, feb./1997, pg.808-810.

[11] - R.J. Bäuerle *et. all*, "Picosecond infrared spectroscopy of hot carriers in a modulation-doped Ga 0..47 In 0.53As multiple-quantum-well structure" – *Physical Review B*, Vol.38, Nº 6, aug./1988, pg. 4307-4310.

[12] - J. M. Wiesenfeld *et. all*, "High-speed multiple quantum well optical power amplifier", *IEEE Photon. Techn. Letters*, Vol. 4, Nº 7, jul./1992**,** pg. 708-711.

[13] - A. Reale *et. all*, "Study of gain compression mechanisms in multiple-quantum-well $In_{1-x}Ga_xAs$ semiconductor optical amplifiers", *IEEE J. of Quantum Electr.*, Vol. 35, Nº 11, novembro/1999, pág. 1697-1703